Supporting Information – Computational Exploration of the Direct Reduction of CO_2 to CO Mediated by Alkali and Alkaline Earth Metal Chloride Anions

Joakim S. Jestilä and Einar Uggerud*

Department of Chemistry and Hylleraas Centre for Quantum Molecular Sciences, University of Oslo, P. O. Box 1033 Blindern, N-0315 OSLO, Norway

SI-A. Data relevant for Born Haber cycles

Table SI-1A. Born Haber cycle parameters and estimated "experimental" enthalpies ($\Delta H^\circ_{rxn,\,MP2}$) for M^- + CO_2 → MO^- + CO in kJ/mol. Experimental ΔH°_f (M(g)), ΔH°_f (MO(g)), ΔH°_f (CO_2(g)) and ΔH°_f (CO(g)) retrieved from thermochemical tables (NIST-JANAF).[1] Computational adiabatic electron affinities (EA_{MP2}) and bond dissociation (ZPE + EE) energies (BDE_{MP2}) from the [MP2/def2-TZVPPD] level of theory. Values from or based exclusively on literature, computational and experimental, in **bold**. Estimates based on a combination of literature values and MP2 calculations in normal text.

	Li	**Na**	**K**	**Rb**	**Cs**	**BeCl**	**MgCl**	**CaCl**	**SrCl**	**BaCl**
$\Delta H^\circ_{f,\,298K}$ (M(g))	**159.3**	**107.5**	**89.0**	**80.9**	**76.5**	**60.7**	**−43.5**	**−104.6**	**−123.8**	**−142.3**
$\Delta H^\circ_{f,\,0K}$ (M(g))	**157.7**	**107.5**	**89.9**	**82.2**	**78.0**					
EA_{MP2}(M)	9.1	22.3	23.8	26.2	28.0	85.7	125.0	101.1	99.6	83.2
EA(M)	**60** [g]	**53** [h]	**48** [i]	**46** [j]	**46** [k]		**153.3** [l]			
$\Delta H^\circ_{f,\,MP2}(M^-(g))$[a]	150.2	85.2	65.2	54.7	48.5	−25.0	−168.5	−205.7	−223.4	−225.5
$\Delta H^\circ_{f,\,298K}$ (M^-(g))[1b]	**99.3**	**54.5**	**41**	**34.9**	**30.5**		**−196.8**			
$\Delta H^\circ_{f,\,0K}$ (M^-(g))[2b]	**97.7**	**54.5**	**41.9**	**36.2**	**32.0**					
$\Delta H^\circ_{f,\,298K}$ (MO(g))*	**84.1**	**83.7**	**71.1**	**59.0** [m]	**62.8**	**136.4**	**58.2**	**43.9**	**−13.4**	**−123.8**
BDE_{MP2}(Cl—MO)	*n.a.*	*n.a.*	*n.a.*	*n.a.*	*n.a.*	279.6	394.6	353.3	324.7	258.7
BDE(M—O)	**333.5**	**256.1**	**277.8**	**255**	**295.8**					
EA_{MP2}(MO)	74.1	99.3	112.5	115.6	108.1	345.5	258.5	226.3	207.2	228.6
EA(MO)	**40.1** [n]	**52.4** [n]	**39.0** [n]	42.8**	**26.3** [o]					
$\Delta H^\circ_{f,\,MP2}(MO^-(g))$[c]	10.0	−15.6	−41.3	−40.7	−45.4	−367.7	−474.0	−414.7	−424.3	−490.1
$\Delta H^\circ_{f,\,298K^1}$ (MO^-(g))[1d]	**44.0**	**31.3**	**32.1**	16.2	**36.4**					
$\Delta H^\circ_{f,\,298K^2}$ (MO^-(g))[2d]	**34.7**	**48**	**21.2**	32.1	**3.4**					
$\Delta H^\circ_{f,\,0K^2}$ (MO^-(g))[2d]	**33.1**	**48.0**	**22.1**	33.4	**4.9**					

$\Delta H^\circ_{rxn,\,MP2}$[e]	142.7	182.1	176.4	187.5	189.1	−59.7	−22.5	74.0	82.1	18.3
$\Delta H^\circ_{rxn,\,298K}$[1] [1f]	**227.6**	**259.7**	**274.1**	264.2	**288.9**					
$\Delta H^\circ_{rxn,\,298K}$[2] [2f]	**218.3**	**276.4**	**263.1**	280.1	**255.8**					
$\Delta H^\circ_{rxn,\,0K}$[2] [2f]	**214.7**	**272.8**	**259.5**	276.5	**252.2**					
$\Delta H^\circ_{f,\,298K}$ (CO_2(g))	**−393.5**									
$\Delta H^\circ_{f,\,0K}$ (CO_2(g))	**−393.1**									
$\Delta H^\circ_{f,\,298K}$ (CO(g))	**−110.5**									
$\Delta H^\circ_{f,\,0K}$ (CO(g))	**−113.8**									
BDE(Cl_2)	**242.0**									
BDE(O_2)	**498.0**									

***** ΔH°_f of the metal oxide without chloride

****** CCSD(T)/def2-TZVPPD (this work)

[g] From ref 2

[h] From ref 3

[i] From ref 4

[j] From ref 5

[k] From ref 6

[l] From ref 7

[m] From ref 8

[n] From ref 9

[o] From ref 10

[a] $\Delta H^\circ_{f,\,MP2}(M^-(g)) = \mathbf{\Delta H^\circ_{f,\,298K}(M(g))} - EA_{MP2}(M)$

[1b] $\mathbf{\Delta H^\circ_{f,\,298K}(M^-(g)) = \Delta H^\circ_{f,\,298K}(M(g)) - EA(M)}$

[2b] $\mathbf{\Delta H^\circ_{f,\,0K}(M^-(g)) = \Delta H^\circ_{f,\,0K}(M(g)) - EA(M)}$

For M = Li – Cs:

[c] $\Delta H^\circ_{f,\,MP2}(MO^-(g)) = \mathbf{\Delta H^\circ_{f,\,298K}(MO(g))} - EA_{MP2}(MO)$

For M = BeCl – BaCl:

[c] $\Delta H^\circ_{f,\,MP2}(MO^-(g)) = \mathbf{\Delta H^\circ_{f,\,298K}(MO(g))} + \frac{1}{2}\,\mathbf{BDE(Cl_2)} - BDE_{MP2}(Cl—MO) - EA_{MP2}(MO)$

[1d] $\mathbf{\Delta H^\circ_{f,\,298K}{}^{1}\,(MO^-(g)) = \Delta H^\circ_{f,\,298K}\,(MO(g)) - EA(MO)}$

[2d] $\mathbf{\Delta H^\circ_{f,\,0K/298K}{}^{2}\,(MO^-(g)) = \Delta H^\circ_{f,\,0K/298K}\,(M(g)) + \tfrac{1}{2}\,BDE(O_2) - BDE(M{-}O) - EA(MO)}$

[e] $\Delta H^\circ_{rxn,\,MP2} = [\Delta H^\circ_{f,\,MP2}\,(MO^-(g)) + \mathbf{\Delta H^\circ_{f,\,298K}\,(CO(g))}] - [\Delta H^\circ_{f,\,MP2}\,(M^-(g)) + \mathbf{\Delta H^\circ_{f,\,298K}\,(CO_2(g))}]$

[1f] $\mathbf{\Delta H^\circ_{rxn,\,298K}{}^{1} = [\Delta H^\circ_{f,\,298K}\,(MO^-(g)) + \Delta H^\circ_{f,\,298K}\,(CO(g))] - [\Delta H^\circ_{f,\,298K}\,(M^-(g)) + \Delta H^\circ_{f,\,298K}\,(CO_2(g))]}$

[2f] $\mathbf{\Delta H^\circ_{rxn,\,0K/298K}{}^{2} = [\Delta H^\circ_{f,\,0K/298K}\,(MO^-(g)) + \Delta H^\circ_{f,\,0K}\,(CO(g))] - [\Delta H^\circ_{f,\,0K}\,(M^-(g)) + \Delta H^\circ_{f,\,0K}\,(CO_2(g))]}$

SI-B. Additional computational details

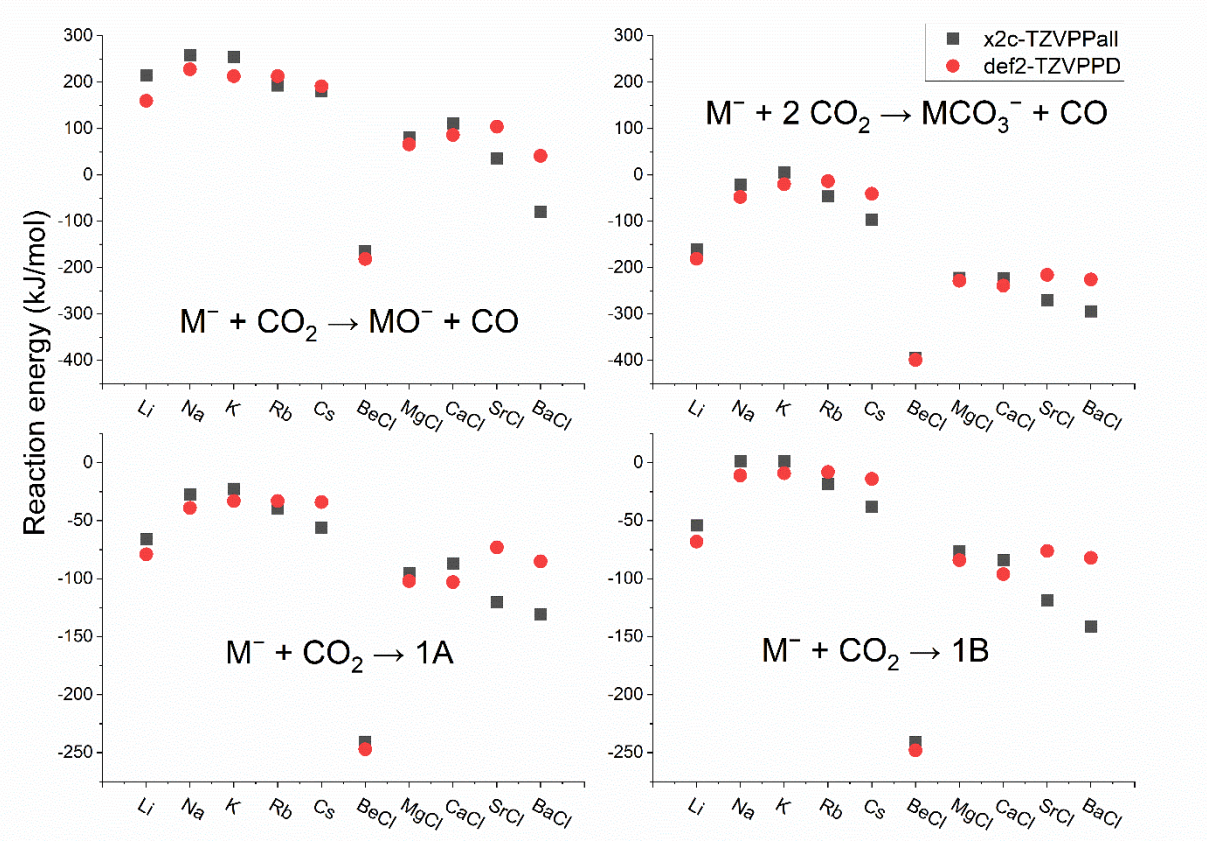

Figure SI-1. Reaction energies (in kJ/mol) for the pseudopotential [MP2/def2-TZVPPD] and all-electron [MP2/x2c-TZVPPall] treatments.

The pseudopotential [MP2/def2-TZVPPD] and the all-electron [MP2/x2c-TZVPPall] treatments for the reduction of both one and two CO_2 to CO are compared in Figure SI-1, and the corresponding numbers are presented in Table SI-1B. The all-electron treatment slightly increases the endothermicity of the reactions for M = Li – K and M = BeCl – MgCl, while decreasing it for the heavy elements M = Rb – Cs and M = SrCl – BaCl compared to the pseudopotential treatment. We assume that this is due to the lower flexibility of the all-electron basis set for the lighter elements, having fewer diffuse basis functions, whereas it is more flexible for the heavier elements, which have moderately diffuse functions and accessible inner shells. Notwithstanding, the periodic trends are qualitatively the same, with decreasing

exothermicity when going down towards the middle of the groups, followed by an increase towards the heavy elements. It is worth noting that this leads to the $M^- + CO_2 \rightarrow MO^- + CO$ reaction for M = BaCl being exothermic with the all-electron treatment, whereas it is slightly endothermic with the pseudopotential treatment.

Table SI-1B. Relative ZPVE-corrected [MP2/def2-TZVPPD] (**def2**) and [MP2/x2c-TZVPPall] (**x2c**) electronic energies in kJ/mol.

		Li	**Na**	**K**	**Rb**	**Cs**	**BeCl**	**MgCl**	**CaCl**	**SrCl**	**BaCl**
M^- + 2 CO_2	**def2**	0*	0*	0*	0*	0*	0	0	0	0	0
	x2c	0*	0*	0*	0*	0*	0	0	0	0	0
1A + CO_2	**def2**	−79*	−39*	−33*	−33*	−34*	−247	−102	−103	−73	−85
	x2c	−66	−27	−23	−40	−56	−240	−95	−87	−120	−131
1B + CO_2	**def2**	−68*	−11*	−9*	−8*	−14*	−248	−84	−96	−76	−82
	x2c	−54	1	1	−18	−38	−241	−77	−84	−118	−141
MO^- + CO	**def2**	160	228	213	213	191	−181	66	86	104	41
	x2c	214	258	254	193	181	−165	80	111	36	−79
MCO_3^- + CO	**def2**	−181	−48	−20	−14	−41	−399	−228	−239	−216	−226
	x2c	−161	−21	5	−46	−97	−394	−222	−223	−270	−294

* from reference [11]

The calculations above and those described in the main text generally follow the frozen core formalism introduced therein, that is C, O, Li, Be, Mg = [$1s^2$]; Na = [$1s^2 2s^2$]; Cl, Ca = [$1s^2 2s^2 2p^6$]; and K = [$1s^2 2s^2 2p^6 3s^2$]. For the heavier elements, Rb, Sr, Cs and Ba in the def2-TZVPPD basis set, all electrons not described by the pseudopotential are correlated, while the frozen cores for these metals in x2c-TZVPPall are adjusted to Rb, Sr = [$1s^2 2s^2 2p^6 3s^2 3p^6$], and for Cs, Ba = [$1s^2 2s^2 2p^6 3s^2 3p^6 4s^2 3d^{10} 4p^6$]. Hence, to elucidate the errors associated with the use of these limited correlation spaces, denoted **FC**, we computed the corresponding full-correlation space energies for a subset of reactions, denoted **Full**. This was done for the x2c-TZVPPall basis set due to its core-electron availability, enabling comparison between

computations involving all electrons for the heavier elements, not solely those not described by the pseudopotential.

Table SI-2B. Relative ZPVE-corrected [MP2=Full/x2c-TZVPPall] and [MP2=FC/x2c-TZVPPall] electronic energies in kJ/mol, denoted **Full** and **FC**, respectively.

		Li	**Na**	**K**	**Rb**	**Cs**	**BeCl**	**MgCl**	**CaCl**	**SrCl**	**BaCl**
M$^-$ + 2 CO_2	**FC**	0	0	0	0	0	0	0	0	0	0
	Full	0	0	0	0	0	0	0	0	0	0
1A + CO_2	**FC**	−66	−27	−23	−40	−56	−240	−95	−87	−120	−131
	Full	−66	−26	−22	−40	−57	−240	−93	−86	−120	−134
1B + CO_2	**FC**	−54	1	1	−18	−38	−241	−77	−84	−118	−141
	Full	−55	2	1	−19	−40	−242	−75	−83	−120	−146
MO$^-$ + CO	**FC**	214	258	254	193	181	−165	80	111	36	−79
	Full	216	261	256	195	179	−163	84	114	35	−83
MCO_3^- + CO	**FC**	−161	−21	5	−46	−97	−394	−222	−223	−270	−294
	Full	−160	−19	6	−47	−99	−393	−219	−222	−270	−298

Finally, we compared MP2 with CCSD(T) and B3LYP (using the def2-TZVPPD basis set) for a selection of reactions to elucidate trends across methods, Table SI-3B. The energies are based on geometries optimized at each respective level of theory.

Table SI-3B. Relative ZPVE-corrected [MP2/def2-TZVPPD], [B3LYP/def2-TZVPPD] and [CCSD(T)=Full/def2-TZVPPD] optimized electronic energies in kJ/mol.

		Li	**Na**	**K**	**Rb**	**Cs**	**BeCl**	**MgCl**	**CaCl**	**SrCl**	**BaCl**
M$^-$ + $2CO_2$	**MP2**	0*	0*	0*	0*	0*	0	0	0	0	0
	B3LYP	0	0	0	0	0	0	0	0	0	0
	CCSD(T)	0	0	0	0	0	0	0	0	0	0
1A + CO_2	**MP2**	−79*	−39*	−33*	−33*	−34*	−247	−102	−103	−73	−85
	B3LYP	−87	−15	−8	−1	−1	−247	−92	−119	−88	−77
	CCSD(T)										
1B + CO_2	**MP2**	−68*	−11*	−9*	−8*	−14*	−248	−84	−96	−76	−82
	B3LYP	−79	*n.e.*	*n.e.*	*n.e.*	*n.e.*	−248	−70	−111	−83	−77

	CCSD(T)										
MO^- + CO	**MP2**	160	228	213	213	191	−181	66	86	104	41
	B3LYP	195	316	331	344	291	−167	111	84	118	77
	CCSD(T)	201	263	233	262	233	−160	93	116	134	70
MCO_3^- + CO	**MP2**	−181	−48	−20	−14	−41	−399	−228	−239	−216	−226
	B3LYP	−183	−33	−17	6	−30	−385	−196	−238	−203	−199

* from reference [11]

Table SI-4B. [MP2/x2c-TZVPPall] NBO partial charges on the reactants, intermediates and products of the $M^- + CO_2 \rightarrow MO^- + CO$ reaction.

		Li	**Na**	**K**	**Rb**	**Cs**	**BeCl**	**MgCl**	**CaCl**	**SrCl**	**BaCl**
M^-	**M**	−1.0	−1.0	−1.0	−1.0	−1.0	0.0	0.0	0.0	0.0	0.0
	Cl	*n.a.*	*n.a.*	*n.a.*	*n.a.*	*n.a.*	−1.0	−1.0	−1.0	−1.0	−1.0
1A	**M**	0.1	−0.2	−0.2	−0.2	−0.2	1.6	1.7	1.8	1.8	1.8
	C	0.7	0.8	0.9	0.9	0.8	0.4	0.4	0.4	0.4	0.4
	O	−0.9	−0.8	−0.8	−0.8	−0.8	−1.1	−1.1	−1.1	−1.1	−1.1
	Cl	*n.a.*	*n.a.*	*n.a.*	*n.a.*	*n.a.*	−0.8	−0.9	−1.0	−1.0	−1.0
1B	**M**	0.0	−0.4	−0.4	−0.3	−0.3	1.5	1.5	1.6	1.6	1.7
	C	0.8	1.0	1.0	0.9	0.9	0.3	0.3	0.3	0.3	0.2
	O_{Bridge}	−1.0	−0.9	−0.8	−0.9	−0.9	−1.1	−1.1	−1.1	−1.1	−1.1
	$O_{Terminal}$	−0.8	−0.7	−0.7	−0.7	−0.7	−0.8	−0.8	−0.8	−0.8	−0.8
	Cl	*n.a.*	*n.a.*	*n.a.*	*n.a.*	*n.a.*	−0.8	−0.9	−0.9	−1.0	−1.0
MO^-	**M**	0.8	0.3	0.3	0.4	0.6	1.6	1.7	1.7	1.7	1.5
	O	−1.8	−1.3	−1.3	−1.4	−1.6	−1.7	−1.8	−1.8	−1.7	−1.6
	Cl	*n.a.*	*n.a.*	*n.a.*	*n.a.*	*n.a.*	−0.8	−0.9	−1.0	−1.0	−1.0

SI-C. Optimized [MP2/def2-TZVPPD] geometries for MCO_2^-, MO^- and MCO_3^-

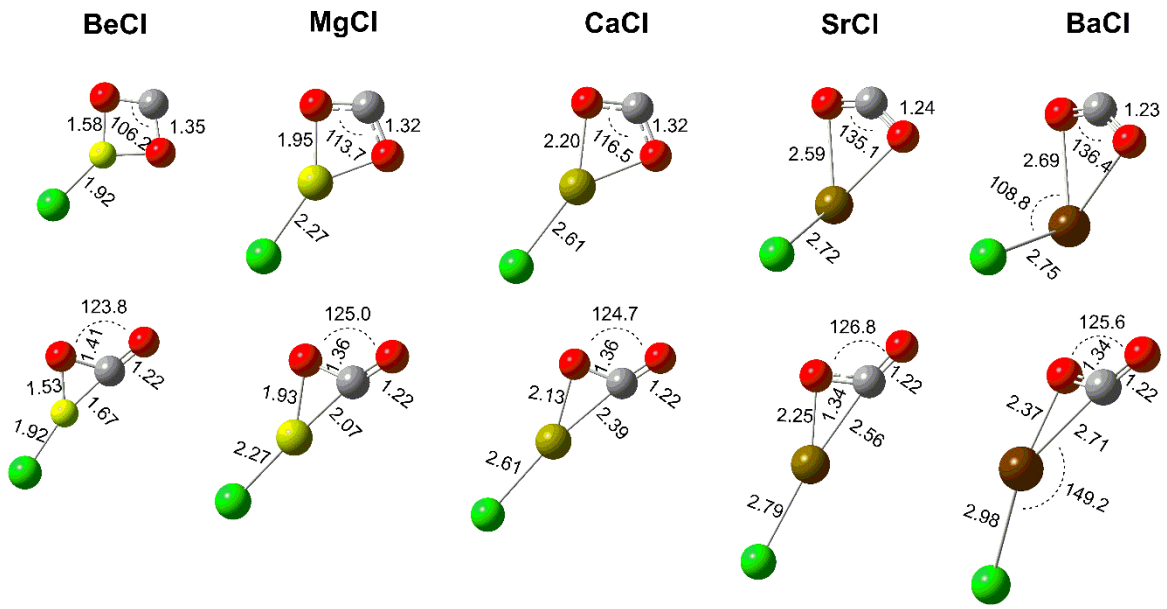

Figure SI-2. [MP2/def2-TZVPPD] optimized MCO_2^- geometries (**1A** on top, **1B** below). The corresponding alkali metal series is reported in reference 11.

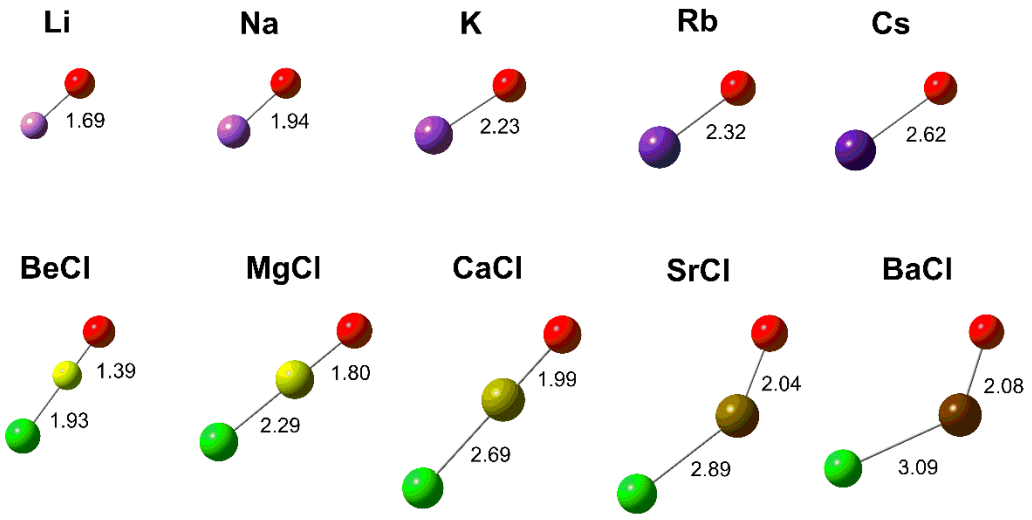

Figure SI-3. [MP2/def2-TZVPPD] optimized MO^- geometries.

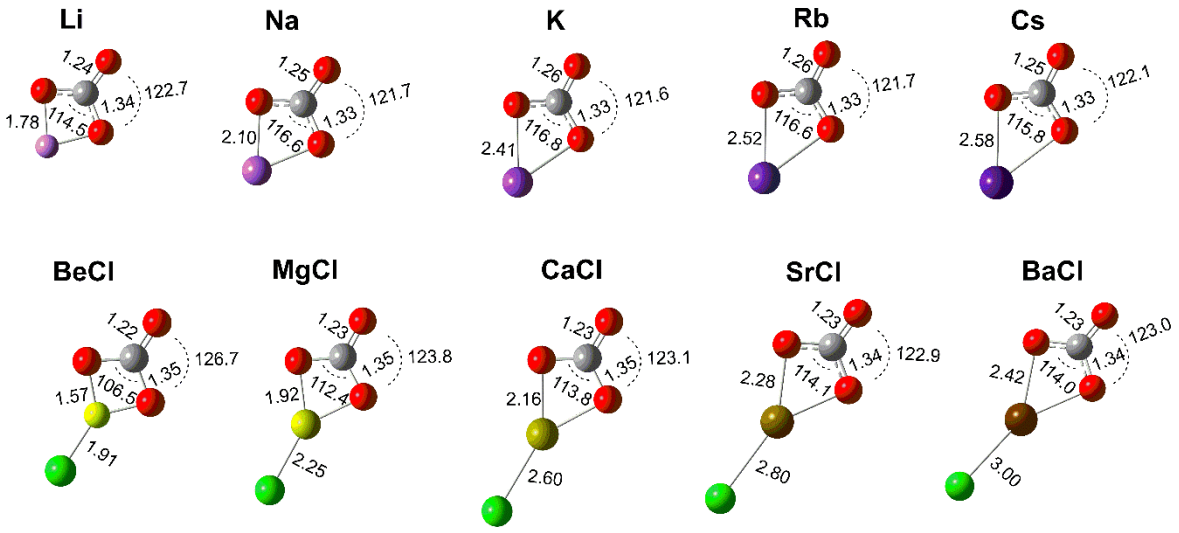

Figure SI-4. [MP2/def2-TZVPPD] optimized MCO_3^- geometries.

SI-F. References

(1) Chase, M. *NIST-JANAF Thermochemical Tables, 4th Edition*; American Institute of Physics, -1, 1998.

(2) Haeffler, G.; Hanstorp, D.; Kiyan, I.; Klinkmüller, A. E.; Ljungblad, U.; Pegg, D. J. Electron Affinity of Li: A State-Selective Measurement. *Phys. Rev. A* **1996**, *53* (6), 4127–4131.

(3) Hotop, H.; Lineberger, W. C. Binding Energies in Atomic Negative Ions: II. *J. Phys. Chem. Ref. Data* **1985**, *14* (3), 731–750.

(4) Andersson, K. T.; Sandström, J.; Kiyan, I. Yu.; Hanstorp, D.; Pegg, D. J. Measurement of the Electron Affinity of Potassium. *Phys. Rev. A* **2000**, *62* (2), 022503.

(5) Frey, P.; Breyer, F.; Holop, H. High Resolution Photodetachment from the Rubidium Negative Ion around the Rb($5p_{1/2}$) Threshold. *J. Phys. B At. Mol. Phys.* **1978**, *11* (19), L589–L594.

(6) Scheer, M.; Thøgersen, J.; Bilodeau, R. C.; Brodie, C. A.; Haugen, H. K.; Andersen, H. H.; Kristensen, P.; Andersen, T. Experimental Evidence That the $6s6p^3$ States of Cs^- Are Shape Resonances. *Phys. Rev. Lett.* **1998**, *80* (4), 684–687.

(7) Miller, T. M.; Lineberger, W. C. Electron Affinity Of MgCl. *Chem. Phys. Lett.* **1988**, *146* (5), 364–366.

(8) Lamoreaux, R. H.; Hildenbrand, D. L. High Temperature Vaporization Behavior of Oxides. I. Alkali Metal Binary Oxides. *J. Phys. Chem. Ref. Data* **1984**, *13* (1), 151–173.

(9) Mintz, B.; Chan, B.; Sullivan, M. B.; Buesgen, T.; Scott, A. P.; Kass, S. R.; Radom, L.; Wilson, A. K. Structures and Thermochemistry of the Alkali Metal Monoxide Anions, Monoxide Radicals, and Hydroxides. *J. Phys. Chem. A* **2009**, *113* (34), 9501–9510.

(10) Sarkas, H. W.; Hendricks, J. H.; Arnold, S. T.; Slager, V. L.; Bowen, K. H. Measurement of the X $^2\Sigma^+$–A $^2\Pi$ Splitting in CsO via Photoelectron Spectroscopy of CsO^-. *J. Chem. Phys.* **1994**, *100* (4), 3358–3360.

(11) Jestilä, J. S.; Denton, J. K.; Perez, E. H.; Khuu, T.; Aprà, E.; Xantheas, S. S.; Johnson, M. A.; Uggerud, E. Characterization of the Alkali Metal Oxalates ($MC_2O_4^-$) and Their Formation by CO_2 Reduction via the Alkali Metal Carbonites (MCO_2^-). *Phys. Chem. Chem. Phys.* **2020**, *22* (14), 7460–7473.